厚生労働科学研究費補助金（創薬基盤推進研究事業）

分担研究報告書

機能性核酸複合体を利用した細胞内核酸の高感度イメージングに関する基礎研究

研究分担者　井原敏博　（熊本大学 大学院自然科学研究科 教授）

研究要旨

両末端にEDTA（ethylenediaminetetraacetic acid）とphen（1,10-phenanthrorine）を化学修飾したDNAコンジュゲートを合成した。このDNAは分子内でヘアピン構造を形成し、その構造において近接した両修飾基は希土類金属を捕捉し、協同的に発光性の錯体を形成する。コンジュゲートのループ部分に相補的なDNAとの二本鎖形成によりこの構造は可逆的に壊れる。この原理を利用して希土類金属錯体の発光を利用したATPセンサーを開発することができた。

共同研究者

北村裕介（熊本大学大学院自然科学研究科）

A. 研究目的

Eu^{3+}や Tb^{3+}などの希土類金属錯体の発光は、バーコード状の特徴的なかたちを与え、その寿命が長く、また、Stokes シフトが大きいという特長を有しているため、時間分解測定法により非常に高感度で計測することが可能である。これらの錯体形成に利用されてきた配位子は、希土類金属イオンをしっかりと捕捉するためのハードは配位子と、励起エネルギーを吸収して金属イオンに伝える役割を果たすアンテナ部位から成る。我々は、配位子をこれら２つの構造要素に分割し、それぞれを別々の DNA 末端に化学修飾したスプリット型のプローブを提案した。両スプリットプローブに相補的なテンプレート存在下、構造要素がテンプレート上で集積して発光性の錯体を形成する有効な環境が再構成され、強発光性の錯体が形成することを報告してきた。本研究では、より洗練されたプローブを目指して、これら２つの構造要素を一つの DNA の両末端にそれぞれ化学修飾した DNA コンジュゲートをプローブ（LCMB: lanthanide complex molecular beacon）として合成した。LCMB は希土類金属イオン（Ln^{3+}: Eu^{3+} or Tb^{3+}）共存下、ヘアピン構造を形成し、その末端で発光性錯体を形成することが期待される。この発光は、LCMB のコンフォメーションに影響を与えるすべての化学的、物理的刺激に応じて変化するだろう。ここでは、一例として ATP センサーの開発を行った。

B. 研究方法

以前のスプリットプローブの研究から、金属捕捉部位、およびアンテナ部位としては、それぞれEDTA （ ethylenediaminetetraacetic acid ） と phen （1,10-phenanthrorine） が有効に機能することがわかっている。本研究では、Schemeにしたがって、これらの分子を、両末端に数塩基の互いに相補的な塩基配列をもつヘアピン構造形成可能なDNAの両末端に導入した。両末端にアミノ基を修飾したDNAを合成し、保護基を選択的に除去しながら、まず3'-末端をphen活性エステルで、つづいて5'-末端はEDTAの酸無水物を用いて修飾し、LCMB

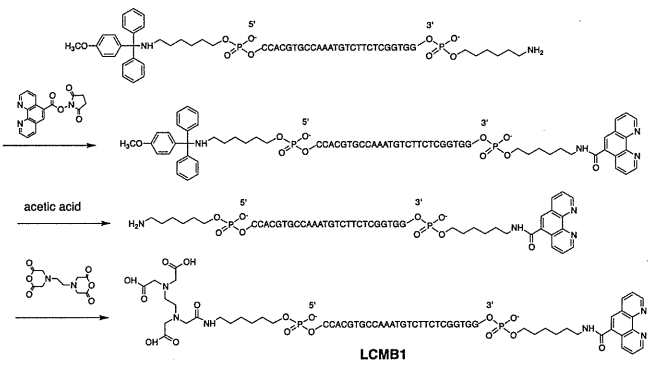

Scheme. LCMB の合成

を得た。MALDI-TOF MSにより同定した。

はじめに、**LCMB1**のループ部分に相補的なDNA、および一塩基を置換したDNAを用いてLn^{3+}/**LCMB1**の発光挙動に与える影響等の基礎的な検討を行った。

つづいて、ATPセンシングの検討を行った。ここではATPアプタマー、**iATP**をATP認識のためのインターフェースとして使用し、**LCMB2**のループ部分は**iATP**と相補的であるように設計している。ATPの検出原理は以下のとおりである。まず測定に先立ち、Ln^{3+}/**LCMB2**/**iATP**の二本鎖を形成させる。このとき、二本鎖形成により**LCMB2**は全体的に伸びるため、phenはLn^{3+}-EDTA錯体と分断され発光は消える。ここに、ATPが添加されると上記二本鎖から**iATP**を奪い、結果としてリリースされた**LCMB2**は発光活性なヘアピン構造をとる。二本鎖形成の可逆性、Ln^{3+}結合の定量的評価を行った後、ATPを含む４種類のNTP（ヌクレオチド-5'-三リン酸、ATP、GTP、CTP、UTP）を添加して発光を観察した。発光の観察はすべて時間分解測定法（delay time: 50 μs; gate time: 2.0 ms）により行った。

C. 研究結果

LCMB1を用いて、センサー素子として重要になる種々の性能に関する基礎的検討を行った。用いたDNAの塩基配列をFigure 1に示す。Figure 2には、Tb^{3+}/**LCMB1**、およびEu^{3+}/**LCMB1**に相補鎖を添加した際の発光スペクトルと、溶液の発光イメージを示した。量子収率は$\phi_{Tb} = 0.17$、$\phi_{Eu} = 0.10$と比較的高く、それぞれ、緑と赤で強く発光し肉眼でも容易に確認することができた。また、**LCMB1**とEu^{3+}との結合定数を求めた結果、$5.0 \times 10^6\ M^{-1}$（0 °Cにおいて）であった（Figure 3）。すなわち、**LCMB1**はヘアピン構造を形成して、その末端のEDTAとphenが互いに接近

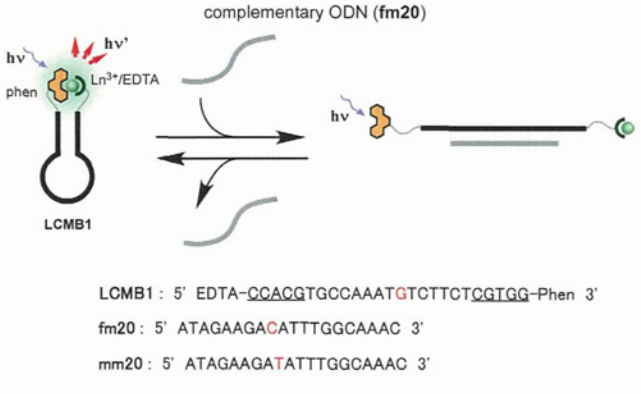

Figure 1. 発光性複合体の可逆的形成反応 **LCMB1**、**fm20**（相補鎖）、**mm20**（含ミスマッチ）の塩基配列

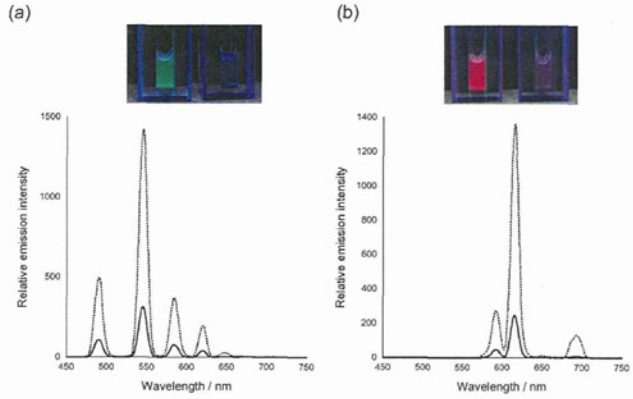

Figure 2. (a) Tb^{3+}/**LCMB1**、および (b) Eu^{3+}/**LCMB1**の発光スペクトル（1.0 μM）　実線、破線はそれぞれ**fm20**存在下、非存在下において計測されたもの。$\lambda_{ex} = 280$ nm、0 °C、。イメージは同溶液の写真。

することが許され、その結果、両リガンドが効率的に発光性の錯体を形成したことがわかった。この発光は、**LCMB1**と等濃度の相補鎖、**fm20**の添加に伴って著しく抑制された。一方、一塩基を置換したDNA、**mm20**を添加した場合には、その発光強度はわずかに10 %減少したのみであり、この結果は、**LCMB1**が高い塩基配列特異性を維持していることを示している。

ここで用いているEu^{3+}/**LCMB1**は、ヘアピン構造で発光on、二本鎖構造で発光offであるので、発シグナルの方向は、従来型のおもに末端修飾基同士のFRETに基づくモレキュラービーコン（MB）とは逆である。この事実から予測されるとおり、Figure 3bに示すように、Eu^{3+}/**LCMB1**、およびEu^{3+}/**LCMB1**/**fm20**のシグナルの温度依存性は、従来型のモレキュラービーコンと完全に上下対称な挙動を示した。温度上昇に伴って、Eu^{3+}/**LCMB1**の発光強度は減少し、80 °Cではほぼ完全に消失した。この変化は融解挙動とよく符

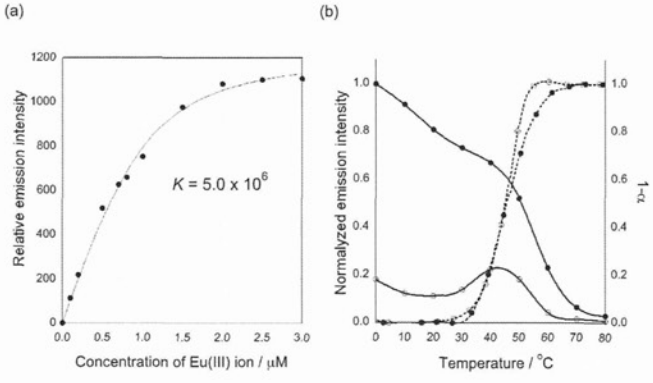

Figure 3. (a) **LCMB1**–Eu^{3+}の滴定曲線および (b) **LCMB1** 複合体の発光の温度特性（実線）と規格化した融解曲線（破線）　●はEu^{3+}/**LCMB1**、○はEu^{3+}/**LCMB1**/**fm20**

合し、温度上昇に伴うヘアピンの融解によって発光性錯体が解離したものと解釈できる。一方、Eu^{3+}/**LCMB1/fm20**の場合には、融解温度付近で極大を与える変化を示した。温度上昇に伴って二本鎖が融解し、一部 Eu^{3+}/**LCMB1**のヘアピン状態となり一旦発光性の錯体を形成するが、続いてすぐに、このヘアピン構造も融解し発光強度は減少する。また、これらの挙動は、温度変化に対してほぼ可逆的であることを確認した。この、LCMBのヘアピン–二本鎖反応に際しての発光挙動の可逆性は次に述べるATPセンサーへの応用のためには必須の条件となる。

Ln^{3+}/LCMBの発光は、相補鎖との結合に伴って減少する。Ln^{3+}/LCMBを特定の分子を標的とするセンサー（イメージング試薬）としてみるとき、この性質は必ずしも魅力的ではない。しかしながら、核酸複合体の形成においては、第三のDNAの関与する競争反応を導入することで、シグナル変化の方向を意図的に反転させることができる。DNAアプタマーは、進化分子工学により取得されたDNAを基体とする分子で、生理活性を持つ小分子からタンパク質まで、特定の分子に特異的に結合する多くのものが知られている。このDNAアプタマーは、DNAとそれ以外の分子を繋ぐインターフェースとみなすことができ、同時に、先述した第三のDNAとしてLn^{3+}/LCMBのシグナル変化の方向を反転させることもできる。すなわち、Ln^{3+}/LCMBは、さまざまなDNAアプタマーの関与する競争反応と組み合わせることで汎用の高感度な発シグナルシステムとなる。

本研究では、生体中のエネルギー通貨であるATP

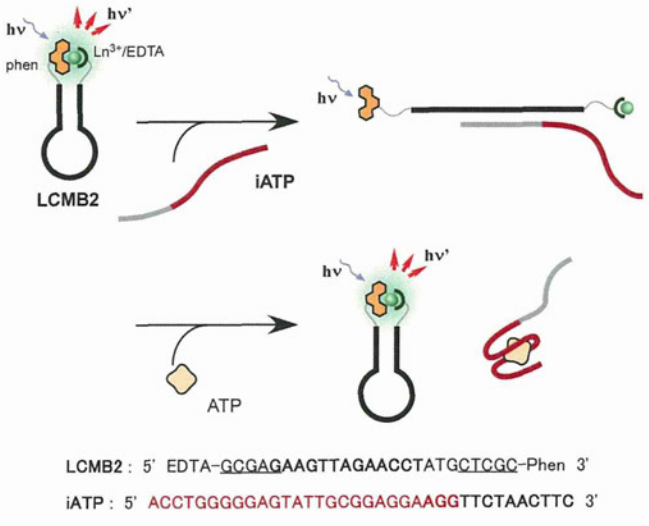

Figure 4. ATP センサーの動作原理　はじめに、Ln^{3+}/**LCMB2** の発光は、**iATP** との二本鎖形成により消光させておく。ここに ATP が添加されると、この二本鎖から競争的に **iATP** が剥がされ、Ln^{3+}/**LCMB2** は再びヘアピン構造をとり、本来の発光を示す。

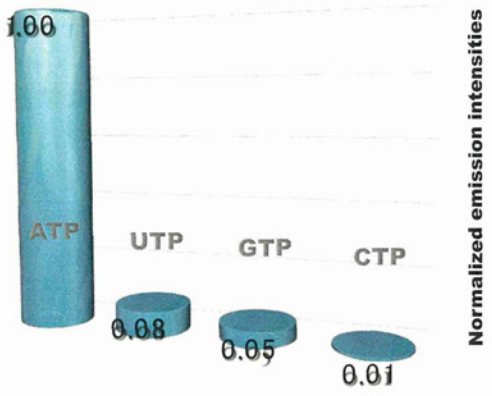

Figure 5. Eu^{3+}/**LCMB2/iATP** を用いた NTP 検出 20 μM NTP を添加し、611 nm の発光強度の相対値を示した（λ_{ex} = 280 nm、0 °C）。

のイメージングを念頭に、Ln^{3+}/**LCMB2**の可逆的コンフォメーション変化に基づく発光on/offの反応を、ATPアプタマー、**iATP**の関与する競争反応を組み合わせてATPセンサーを構築することで、上記イメージング試薬の設計思想を証明したいと考えた。Figure 4には、ATPセンサーの反応スキーム、および用いたDNAの塩基配列を示した。計測に先立って、発光性のEu^{3+}/**LCMB2**に**iATP**を加え、Eu^{3+}/**LCMB2/iATP**二本鎖複合体を形成させて一旦発光を抑える。この系に、ATPが添加されると、競争反応により複合体からiATPが剥がされ、解離したEu^{3+}/**LCMB2**は再び発光性のヘアピン型構造となる。

Eu^{3+}/**LCMB2/iATP**溶液に20 μMの４種のNTPを添加し、時間分解測定法により611 nmの相対発光強度を記録した結果をFigure 5に示す。期待されるとおり、ATPに強く応答し、その他の３種のNTPにはほとんど反応しないことがわかった。

D. 考　察

従来型のMBと逆に、Ln^{3+}/LCMBのシグナルは、ヘアピン状態でon、二本鎖状態でoffとなる。相補鎖の添加によりLn^{3+}/LCMBの発光シグナルは減少、すなわちon-off型の応答であるため、DNA相補鎖の検出法としては決して理想的なものではない。しかしながら、相補鎖の関与するもう一つの競合する特異反応と組み合わせることで、シグナル変化の方向をoff-on型に反転させ、さらに相補鎖としてDNAアプタマーを用いれば、標的分子をDNAやRNA以外の分子に拡張することも可能である。本系では、上記原理にしたがってATPセンサーを構築することでこれを実証することに成功した。検出感度はサブμMレベ

ルとそれほど高いものではないが、酵素反応等のシグナル増幅ステップを用いない単純な分光学的検出系でのATPセンサーとしては最高レベルである。特異性においても、その他のすべてのNTPに対して10倍位以上の高いコントラストを示した。ATPアプタマーの選択性が、Eu^{3+}/**LCMB2/iATP**系での競争反応においても維持されていることを示している。

E. 結　論

Ln^{3+}/LCMBの発光寿命は、τ_{Tb} = 1.26 ms、τ_{Eu} = 1.34 msと充分に長いことが、以前の我々の研究によりわかっている。時間分解測定法を用いて、50 μs (= delay time) 以降の発光強度を積算することで、夾雑物質由来のバックグラウンド蛍光を極度に抑制してシグナルを高感度に計測することが可能となる。本研究において、ATPセンサーの構築をとおして示したように、Ln^{3+}/LCMBは標的とする分子に対するアプタマーが得られていさえすれば、それらをインターフェースとすることで、あらゆる分子のセンサーに適用することができる。すなわち、Ln^{3+}/LCMBは、汎用の高感度発シグナルモジュールとみなすことができる。

F. 健康危険情報

なし

G. 研究発表

1. 論文発表

1) Yusuke Kitamura, Shikinari Yamamoto, Yuka Osawa, Hirotaka Matsuura, Toshihiro Ihara, "Versatile allosteric molecular devices based on reversible formation of luminous lanthanide complexes", *Chemical Communications*, **49**, 285–287 (2013).

2) Toshihiro Ihara, Yusuke Kitamura, "Photochemically relevant DNA-based molecular systems enabling chemical and signal transduction and their analytical applications", *Journal of Photochemistry and Photobiology C: Photochemistry Reviews*, **13**, 148–167 (2012).

3) 井原敏博, 北村裕介, "スプリット型プローブの協同的錯体形成を利用するDNAの認識及び検出", *分析化学*, **61**, 193–206 (2012).

2. 学会発表

1) Toshihiro Ihara, "DNA-directed metal complex formation and analytical applications", Asian International Symposum（招待講演）, 2013 年 3 月 24 日, 草津市

2) Akika Futamura, Yusuke Kitamura, Yusuke Sato, Seiichi Nishizawa, Norio Teramae, Toshihiro Ihara, "Flexible fluorometry for DNA and RNA analysis using rationally combined two probes", The 39th International Symposium on Nucleic Acids Chemistry, 2012 年 11 月 15 日, 名古屋市

3) Yusuke Kitamura, Shikinari Yamamoto, Yuka Osawa, Toshihiro Ihara, "Versatile molecular devices based on the reversible formation of luminous lanthanide complexes", The 39th International Symposium on Nucleic Acids Chemistry, 2012 年 11 月 15 日, 名古屋市

4) 北村裕介, 山元識生, 大澤由佳, 井原敏博, "希土類金属錯体の可逆的形成を利用したアロステリック分子センサーの開発", 第 6 回バイオ関連化学シンポジウム, 2012 年 9 月 26 日, 札幌市

5) Akika Futamura, Takeshi Imoto, Yusuke Kitamura, Seiichi Nishizawa, Yusuke Sato, Norio Teramae, Toshihiro Ihara, "Rationally designed combinations of two molecules for the detection of specific nucleobases", 11th European Biological Inorganic Chemistry Conference, 2012 年 9 月 12 日, Granada

6) Tatsuaki Ishii, Yusuke Kitamura, Toshihiro Ihara, "Silver ion-induced DNA triplex formation under neutral pH conditions", 11th European Biological Inorganic Chemistry Conference, 2012 年 9 月 12 日, Granada

7) Yusuke Kitamura, Shikinari Yamamoto, Yuka Osawa, Mayumi Yamamoto, Yusuke Tsujimura, Toshihiro Ihara, "Cooperative formation of luminescent lanthanide complexes by metal chelator-DNA conjugates and their application to biosensor", 11th European Biological Inorganic Chemistry Conference, 2012 年 9 月 12 日, Granada

8) Toshihiro Ihara, Akika Futamura, Yusuke Kitamura, Yusuke Sato, Seiichi Nishizawa, Norio Teramae, "DNA/RNA probing using rationally selected two DNA ligands", The Second Asian Chemical Biology Conference, 2012 年 7 月 4 日, 糸満市

9) Yusuke Kitamura, Shikinari Yamamoto, Yuka Osawa, Toshihiro Ihara, "Versatile molecular beacons based on the reversible formation of luminous lanthanide complexes", The Second Asian Chemical Biology Conference, 2012 年 7 月 4 日, 糸満市

H. 知的財産権の出願・登録状況

なし

III. 研究成果の刊行に関する一覧表

研究成果の刊行に関する一覧表

雑誌

発表者氏名	論文タイトル名	発表誌名	巻号	ページ	出版年
M. Murata, S. Narahara, K. Umezaki, R. Toita, S. Tabata, J. S. Piao, K. Abe, J.-H. Kang, K.Oouchida, L. Cui, M. Hashizume	Liver cell specific targeting by the preS1 domain of hepatitis B virus surface antigen displayed on protein nanocages	*International Journal of Nanomedicine*	7	4353-4362	2012
R. Toita, M. Murata, S. Tabata, K. Abe, S. Narahara, J. S. Piao, J.-H. Kang, M. Hashizume	Development of Human Hepatocellular Carcinoma Cell-Targeted Protein Cages	*Bioconjugate Chemistry*	23	1494-1501	2012
T. Ihara, Y. Kitamura	Photochemically relevant DNA-based molecular systems enabling chemical and signal transductions and their analytical applications	Journal of Photochemistry and Photobiology C: Photochemistry Reviews	13	148–167	2012
R. Toita, M. Murata, K. Abe, S. Narahara, J. S. Piao, J.-H. Kang, K. Ohuchida, M. Hashizume	Biological evaluation of protein nanocapsules containing doxorubicin	*International Journal of Nanomedicine*	8	1989-1999	2013
Y. Kitamura, S. Yamamoto,a Y. Osawa, H. Matsuuraa, T.Ihara	Versatile allosteric molecular devices based on reversible formation of luminous lanthanide complexes	*Chemical Communications*	49	285–287	2013

IV. 研究成果の刊行物・別刷

International Journal of Nanomedicine

Dovepress

open access to scientific and medical research

Open Access Full Text Article

ORIGINAL RESEARCH

Liver cell specific targeting by the preS1 domain of hepatitis B virus surface antigen displayed on protein nanocages

This article was published in the following Dove Press journal:
International Journal of Nanomedicine
8 August 2012
Number of times this article has been viewed

Masaharu Murata[1,2]
Sayoko Narahara[1,2]
Kaori Umezaki[1]
Riki Toita[1,2]
Shigekazu Tabata[1]
Jing Shu Piao[1]
Kana Abe[1]
Jeong-Hun Kang[3]
Kenoki Ohuchida[1,4]
Lin Cui[4]
Makoto Hashizume[1,2]

[1]Department of Advanced Medical Initiatives, Faculty of Medical Science, Kyushu University, Fukuoka, Japan; [2]Innovation Center for Medical Redox Navigation, Kyushu University, Fukuoka, Japan; [3]Department of Biomedical Engineering, National Cerebral and Cardiovascular Center Research Institute, Osaka, Japan; [4]Department of Surgery and Oncology, Graduate School of Medical Sciences, Kyushu University, Fukuoka, Japan

Abstract: Protein nanocages are self-organized complexes of oligomers whose three-dimensional architecture can been determined in detail. These structures possess nanoscale inner cavities into which a variety of molecules, including therapeutic or diagnostic agents, can be encapsulated. These properties yield these particles suitable for a new class of drug delivery carrier, or as a bio-imaging reagent that might respond to biochemical signals in many different cellular processes. We report here the design, synthesis, and biological characterization of a hepatocyte-specific nanocage carrying small heat-shock protein. These nanoscale protein cages, with a targeting peptide composed of a preS1 derivative from the hepatitis B virus on their surfaces, were prepared by genetic engineering techniques. PreS1-carrying nanocages showed lower cytotoxicity and significantly higher specificity for human hepatocyte cell lines than other cell lines in vitro. These results suggested that small heat-shock protein-based nanocages present great potential for the development of effective targeted delivery of various agents to specific cells.

Keywords: protein nanocages, drug delivery system, hepatocyte cell lines specific, hepatitis B virus

Introduction

As most drugs have both beneficial and unfavorable effects pertaining to chemotherapy, which might also be tissue dependent, it is necessary to deliver therapeutic agents selectively to their target sites.[1–4] Conventional chemotherapeutic agents diffuse non-specifically throughout the body where they affect both malignant and normal cells; unfortunately, 95% of all new potential therapeutics have poor pharmacokinetic and biopharmaceutical properties.[5] To overcome these problems, there is a serious need to develop effective drug delivery systems (DDS) that distribute therapeutically active drug molecules only to the desired site of action without affecting healthy organs and tissues.

Various strategies for site-specific drug delivery have led to the development of drug carriers. In particular, DDS based on liposomes[6,7] and synthetic polymers[8–11] have been extensively studied as novel drug-packaging strategies for cancer chemotherapy. In the last decade, nanotechnological innovations have played an important role in size control and surface modification of nanomaterials, and the resulting properties play a critical role in target specificity for tumor tissues via improved pharmacokinetics and pharmacodynamics and in allowing active intracellular delivery characteristics.[12] Traditional DDS materials, including liposomes and synthetic polymers, can be manufactured in bulk at low cost and with a wide diversity of backbones, surface

Correspondence: Masaharu Murata
Department of Advanced Medical Initiatives, Faculty of Medical Science, Kyushu University, 3-1-1 Maidashi, Higashi-ku, Fukuoka 812-8582, Japan
Tel +81 926 426 251
Fax +81 926 426 252
Email m-murata@dem.med.kyushu-u.ac.jp

submit your manuscript
Dovepress
http://dx.doi.org/10.2147/IJN.S31365

chemistries, and molecular weights; however, their aggregate structure and compositional sequence cannot be accurately controlled and therefore such materials offer disadvantages in their poor responsiveness to cellular behavior that require sequence specificity and structural stringency to be sensitive to signals exhibited by certain cell biochemical processes or states.

On the other hand, natural or recombinant protein-based nanocapsules or nanocages are also being actively investigated as new types of nanomaterial.[13–16] These nanocapsules are self-organized protein oligomer complexes with nanoscale inner cavities and whose three-dimensional architecture can be specified in great detail.[17,18] Thus, they have the potential to offer special advantages in developing new functions that are responsive to biochemical signals exhibited by various cellular processes. Such specific interactions derive from the incorporated amino acid sequences that can be designed to address multiple functional requirements for biomaterial applications. Recently, we constructed stimulus-responsive nanomaterial by incorporating a genetically engineered small heat shock protein (sHSP) that can change its conformation in response to dual stimuli, a protease signal and temperature, in contrast to the wild type.[19]

Here, a novel targeted drug delivery method is presented involving a protein-based nanocage composed of HSP16.5, a sHSP from a hyperthermophilic archaeon.[20–22] This protein forms a 400 kDa homogeneous complex comprised of 24 subunits that self-organizes under physiological conditions to form a nanoscale, hollow, spherical capsule with small pores, contain very high thermal stability, and offer the potential for a variety of molecules, including drugs and magnetic resonance imaging contrast agents, to be encapsulated in the cavity. These unique properties yield HSP16.5 suitable for a drug carrier, but this protein exhibits no significant organ or tissue specificity in body distribution following intravenous administration in mice.[23] To address this problem, a recombinant fusion protein was constructed from HSP16.5 and a target-specific peptide using genetic engineering. Examinations of the crystal structure of the HSP16.5 complex have revealed that the C-terminal region is on the exterior surface of the capsule-like structure.[24] Thus, a recombinant HSP16.5 was designed and produced by an in-frame fusion, with the sequence for a targeting peptide added in this region. Specificity for liver cells-targeted delivery of the nanocapsule was achieved using a preS1 peptide for the targeting peptide (Figure 1).[25–27] This peptide is derived from the envelope proteins of the hepatitis B virus (HBV), with a known affinity for primary hepatocytes and hepatocyte cell lines.[28,29] The mechanism of hepatocyte infection induced by HBV is not absolutely clear; however, specific attachment of viruses to cells is the essential first step in virus entry into cells. Several studies suggested that amino acids 21-47 of preS1 play a major role in the cell attachment.[30–32] For example, Dash et al reported that this 27-mer preS1 peptide (21-47) binds to HepG2 cells in a dose-dependent manner with high affinity.[32] Furthermore, this binding is possibly tissue-specific, since only weak to insignificant levels of binding were obtained with Vero cells, HeLa cells, and human peripheral lymphocytes. This paper describes the characterization of 27-mer preS1 peptide-carrying nanocapsules and their potential for biomedical applications, including targeted drug delivery and bioimaging.

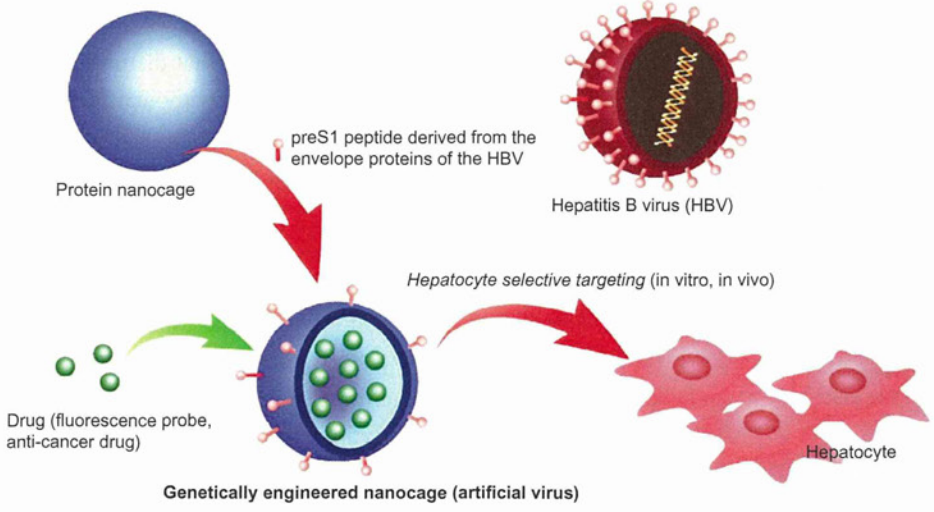

Figure 1 Schematic illustration of genetically engineered nanocages for hepatocyte selective targeting.

Materials and methods

DNA cloning and expression

Plasmid pET-HSPG41C-preS1, a bacterial expression vector containing the *preS1* gene fused in frame with the HSP16.5 variant (HSPG41C), was cloned by polymerase chain reaction (PCR). The HSPG41C mutant presents unique reactive cysteine residues on the interior surface of the assembled cage for the attachment of cargo molecules. This mutant was constructed according to the guidelines noted in a previous paper,[19] and is used as a PCR template. The primers for HSPG41C-preS1 were 5′-taatacgactcactataggg-3′(forward primer), 5′-cgcggatccCTACGGGTTGAAGTCCCAGTC-CGGGTTGTTAGAGTTAGCACCGAAAGCCGGGTC CAGCTGGTGGTCCGGGAAGAAACCCAGCGGGCTA GCttcaatgttgattcctttcttaattgagga-3′ (reverse primer), and the latter primer contained a *preS1* gene coding region (capital letters) and *BamH*I restriction site (underlined). The PCR-generated 0.63-kb fragment was digested with *Nde*I and *BamH*I and the resulting DNA fragment ligated into *Nde*I and *BamH*I-digested pET21a vector (Novagen; Merck Japan, Tokyo, Japan). Correct insertion of the fragment was verified by DNA sequencing and plasmids then amplified and purified by standard techniques.

The resulting vector was allowed to express HSPG41C-preS1 in *Escherichia coli* BL21-Gold(DE3) cells (Novagen) using a T7 expression system. Bacterial cells of BL21 gold (DE3) containing pET-HSPG41C-preS1 were grown in 2 × YT medium (Sigma-Aldrich, St Louis, MO) with 100 mg/mL ampicillin at 37°C. Recombinant protein production was initiated by addition of isopropyl thiogalactopyranoside (IPTG; Wako Pure Chemical Industries, Ltd, Osaka, Japan) to a final 1 mM concentration and incubation at 37°C for 4 hours.

Protein purification and characterization

Cells were pelleted by centrifugation at 4°C, the pellet resuspended in 8 mL of sample buffer (20 mM KH_2PO_4-KOH, pH 7.0, 2 mM DTT, and 1 mM ethylenediaminetetraacetic acid), and the resulting suspension sonicated on ice (200 watts, 45 seconds). DNase 1 and RNase A were then added to final concentrations of 5 and 1 mg/mL, respectively. The cell lysate mixture was incubated at 4°C for 30 minutes, and the insoluble material removed by centrifugation (20,000 g, 20 minutes) at 4°C. Purification of the recombinant protein was performed by ion-exchange chromatography, in which the supernatant was loaded on a HiLoad 26/10 Q Sepharose HP™ anion-exchange column (Amersham Pharmacia Biotech Inc; GE Healthcare, Little Chalfont, UK) and HSPG41C-preS1 eluted with sample buffer containing 1M NaCl. Fractions containing HSPG41C-preS1, confirmed by sodium dodecyl sulfate polyacrylamide gel electrophoresis (SDS-PAGE), were loaded onto a silica-based GPC column TSKgel G3000SW (Tosoh Corporation, Tokyo, Japan) and HSPG41C-preS1 eluted with storage buffer (25 mM NaH_2PO_4/Na_2HPO_4, pH 7.0, and 0.1 M NaCl). The resulting purified HSPG41C-preS1 fractions were analyzed by SDS-PAGE using 12% gel according to standard protocol. The recombinant HSPG41C-preS1 protein cages were characterized by matrix-assisted laser desorption/ionization time-of-flight mass spectrometry (Autoflex Speed; Bruker Daltonics Japan, Yokohama, Japan) and dynamic light scattering (Malvern Nanosizer ZS; Malvern Instruments).

Cytotoxicity assays

HepG2, Huh-7, and HeLa cells were cultured in Dulbecco's Modified Eagle's Medium (DMEM; Wako Pure Chemical Industries, Ltd), supplemented with 1% (v/v) antibiotic-antimycotic mix (Gibco 15240-062; Life Technologies Japan Ltd., Tokyo, Japan) and 10% (v/v) fetal bovine serum (FBS; GE Healthcare, Little Chalfont, UK). MCF-7 cells were cultured in RPMI-1640 (Sigma-Aldrich) with 1% (v/v) antibiotics and 10% FBS and at 37°C in a humidified 5% CO_2 atmosphere.

The cellular toxicity of the nanocages in vitro was assessed using the CellTiter-Glo® luminescent cell viability assay (Promega Corporation, Madison, WI) according to the manufacturer's instructions. This assay is a homogeneous method designed to determine the viable cell numbers in culture based on quantitation of available adenosine triphosphate, signaling the presence of metabolically active cells at the assay end point. Cells (1×10^4 cells/well) were cultured in 96-well microtiter plates in complete growth medium in the presence of increasing nanocapsule concentrations. For chronic toxicity assessment, nanocapsules were applied to cells at various concentrations and incubated for 16 hours prior to assay for viable cells.

Fluorescence assay

Prior to a fluorescence assay, HSPG41C-preS1 and HSPG41C (used as a control) were labeled with fluorescent dye. Briefly, nanocapsules were incubated with a 5-fold molar excess of Alexa488-maleimide (Invitrogen; Life Technologies, Carlsbad, CA) in pH 8.0 phosphate buffer at 50°C overnight and then excess dye removed by ultrafiltration. Uptake or transfection was assessed by

seeding 1×10^4 cells in 100 µL of complete growth medium per well in 96-well microtiter plates 12 hours before nanocage addition, to allow for cell attachment. After cell culture medium exchange, the cells were incubated for various times with dye-labeled nanocapsules at a final 1 µM concentration. In inhibition experiments, synthetic preS1 peptide (PLGFFPDHQLDPAFGANSNNPDWDFNP; final concentration, 25 µM) was added, as a competitive inhibitor, to the culture medium 3 hours prior to nanocage addition. After incubation, the cells were washed twice with phosphate buffered saline, the medium changed to a phenol red-free medium, and dye-labeled nanocapsule cellular uptake quantified using a multilabel counter ARVO MX (PerkinElmer Japan Co., Ltd., Yokohama, Japan) excitation and emission, 485 and 535 nm, respectively. Nanocapsule transfection efficiencies were calculated by dividing the total fluorescence intensity in each well by the total number of viable cells in the well, as determined by the cell viability assay.

For investigating nanocapsule cellular localization, HepG2, Huh-7, HeLa, and MCF-7 cells were seeded at 1×10^4 cells/well in µ-Slides (µ-Slide 6 well; ibidi GmbH, Munich, Germany), incubated with colorless DMEM containing 1% antibiotic-antimycotic mix and 10% FBS (PAA; GE Healthcare) overnight. Then, fluorescent-labeled nanocages of HSPG41C-preS1 or HSPG41C control were added to wells at a final 1 µM concentration and, after additional 6 hours of incubation, non-incorporated nanocapsules removed by washing cells twice with phosphate buffered saline and adding fresh medium. Fluorescence confocal laser scanning microscopy was performed with a Bio-Rad Radiance 2100 confocal laser scanning microscopy system (Bio-Rad Laboratories Japan, Tokyo, Japan) attached to a Nikon TE2000-U microscope (Nikon Corporation, Tokyo, Japan). All fluorescence images were acquired under the same conditions of objective lens, laser excitation intensity, photomultiplier gain, and imaging size. Statistical significances of the differences were determined by Student's *t*-test.

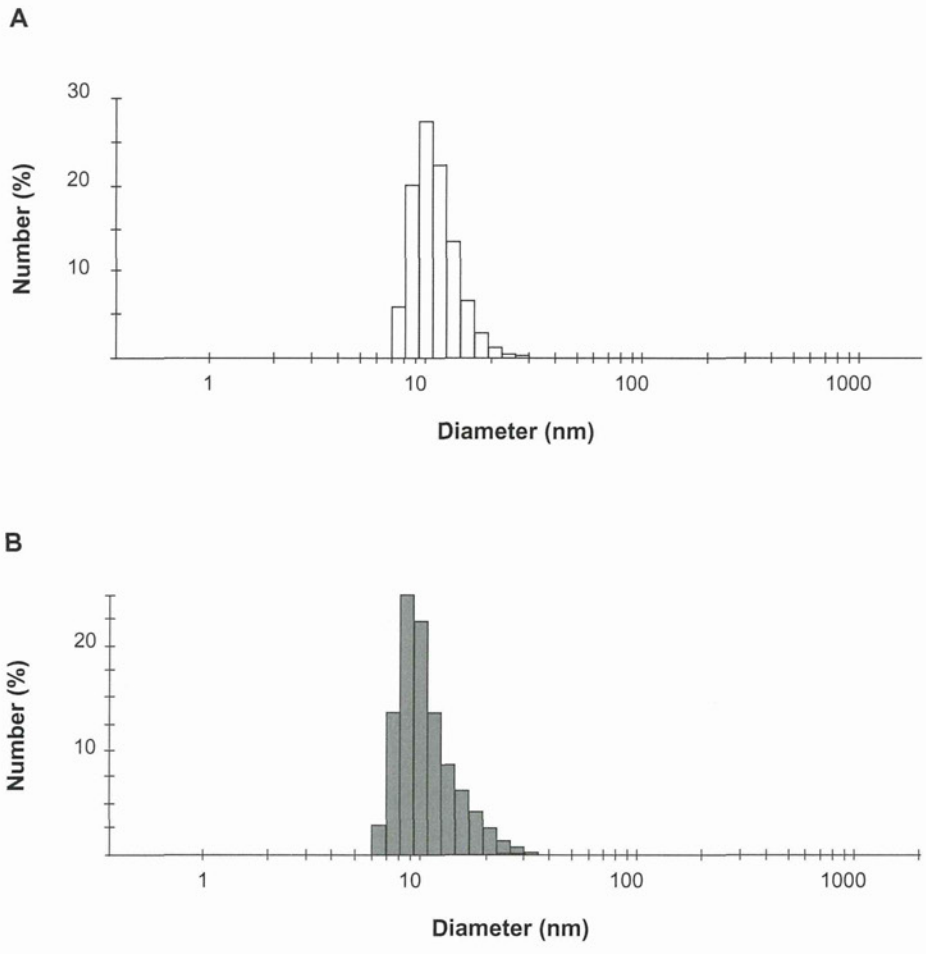

Figure 2 Dynamic light scattering analysis of protein nanocages. (**A**) HSPG41C nanocage controls; (**B**) HSPG41C-preS1 nanocages.

Results and discussion

Expression and characterization of preS1-carrying protein nanocages

Expression vectors encoding the HSPG41C-preS1 or HSPG41C were constructed and recombinant sHSP16.5 proteins produced in *E. coli* BL21-Gold(DE3) and purified by sequential anion exchange chromatography followed by size exclusion chromatography under native conditions (Figure S1). Purified proteins, separated by SDS-PAGE, appeared as a single band by Coomassie blue staining. The observed molecular weight of purified HSPG41C-preS1 (m/z = 19676.2 Da), analyzed by matrix-assisted laser desorption/ionization time-of-flight mass spectrometry with a sinapic acid matrix, was largely in agreement with calculations (m/z = 19668.2 Da) (Figure S2). The protein nanocage size range and distribution were measured by means of dynamic light scattering. These results indicated that the average nanocage diameter of the HSPG41C-preS1 and HSPG41C were 14.4 and 12.7 nm, respectively, with a narrow size distribution (Figure 2). These results demonstrated that HSPG41C-preS1 cages were slightly larger than HSPG41C parent cages lacking the targeting peptide.

In vitro cellular cytotoxicity of nanocages

As cell cytotoxicity is an important factor in selecting materials for drug carriers, the nanocages produced here were characterized regarding their effect on cell viability under the same conditions as used for fluorescence assay of cellular uptake experiments. Neither HSPG41C nor HSPG41C-preS1 had any appreciable cytotoxic effect under these conditions (Figure 3); similar results were obtained from wild type HSP16.5 protein under the same conditions (data not shown). These results showed that the single amino acid substitution mutation, contained in HSPG41C, and the cage surface modification with the

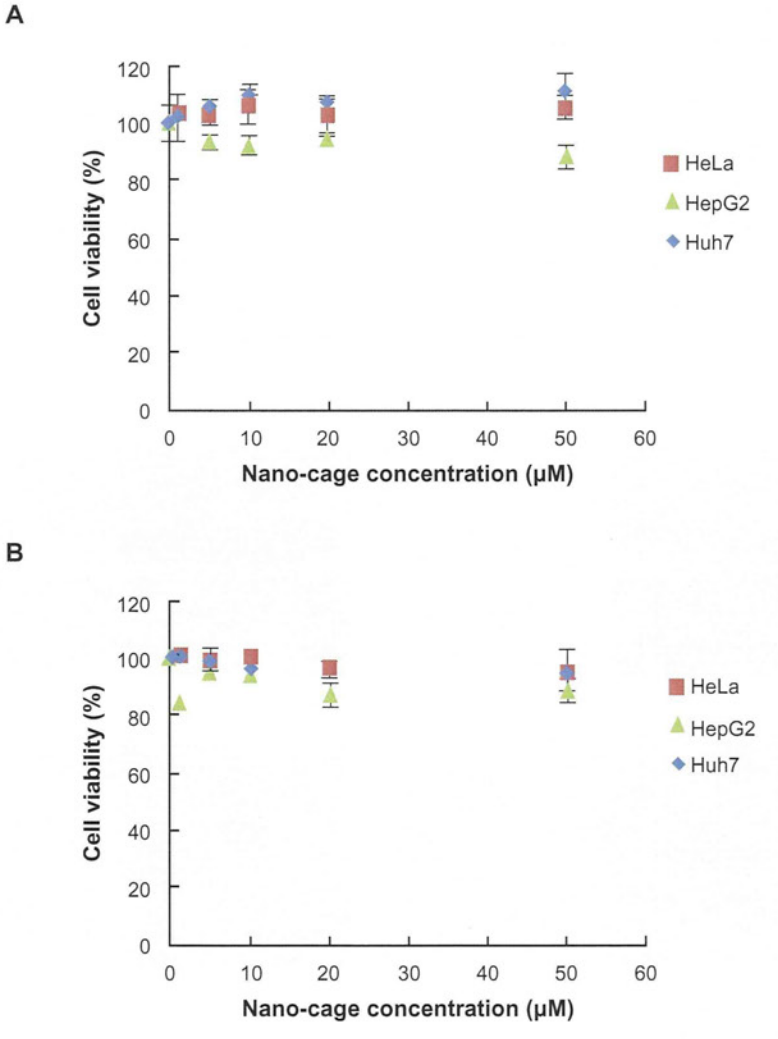

Figure 3 Cell viability measurements after treatment with protein nanocages against various cell lines. (**A**) HSPG41C nanocage controls; (**B**) HSPG41C-preS1 nanocages.

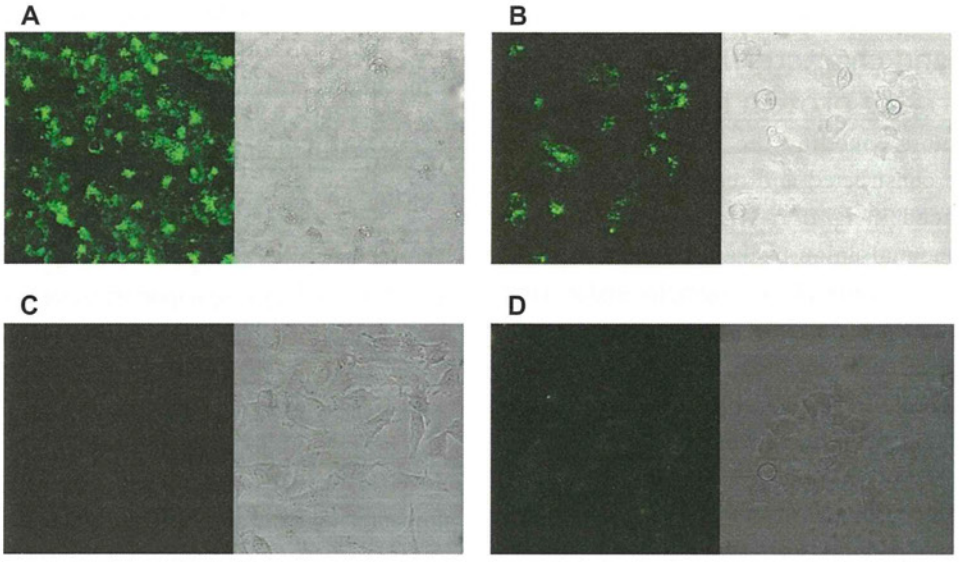

Figure 4 Fluorescence confocal laser scanning microscopy of various cells with fluorescently-labeled HSPG41C-preS1 nanocages. Alexa488-labeled HSPG41C-preS1 nanocages added to culture media with 1×10^4 cells of Huh-7 (**A**), HepG2 (**B**), HeLa (**C**), and MCF7 (**D**), and extensively washed with PBS before CLSM analysis.
Abbreviations: PBS, phosphate buffered saline; CLSM, confocal laser scanning microscopy.

preS1 peptide of wild type HSP16.5, contained on HSPG41C-preS1, did not significantly affect their cytotoxicity.

Hepatocyte specific delivery of protein nanocages in vitro

The mechanism for the entry of HBV particles into target cells, in particular into hepatocytes, is not yet understood. However, the preS1 surface antigen of HBV is known to play an important role in initial HBV attachment to hepatic cell lines, with the preS1 domain N-terminal segment believed to be essential. To demonstrate that preS1 fusion into the HSP16.5 protein nanocage produced a new nanocage binding affinity towards hepatocyte cell lines, the specific target cells of HBV preS1 molecule, transfection assays were performed.

Fluorescent-labeled HSPG41C-preS1 nanocages were observed to efficiently internalize to human hepatoma cell lines HepG2 and Huh-7, which bear specific HBV receptors compared to internalization to the other cell lines (Figure 4). Incubation with these nanocages resulted in specific

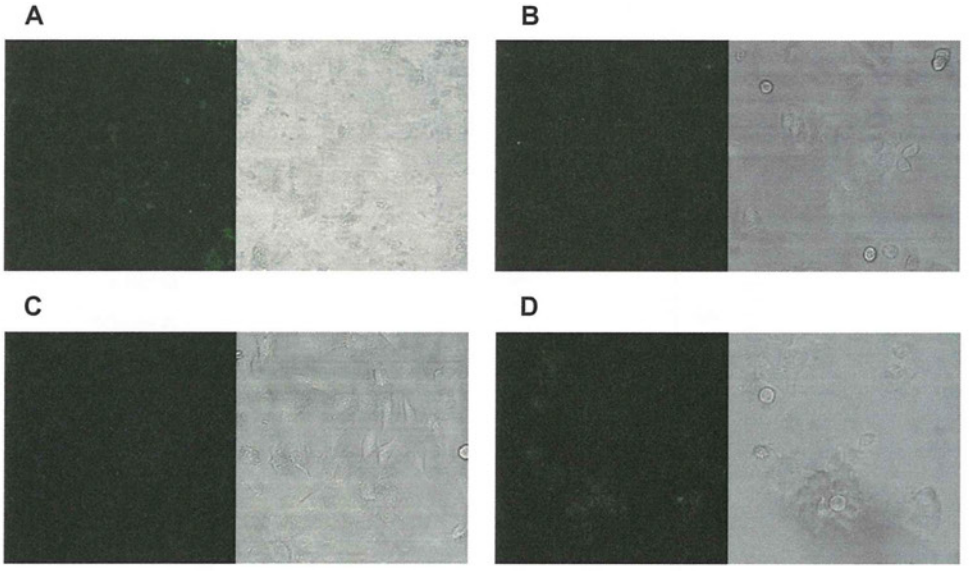

Figure 5 Fluorescence confocal laser scanning microscopy of various cells with fluorescently-labeled HSPG41C nanocages. Alexa488-labeled HSPG41C nanocages added to culture media with 1×10^4 cells of Huh-7 (**A**), HepG2 (**B**), HeLa (**C**), and MCF7 (**D**), and extensively washed with PBS before CLSM analysis.
Abbreviations: PBS, phosphate buffered saline; CLSM, confocal laser scanning microscopy.

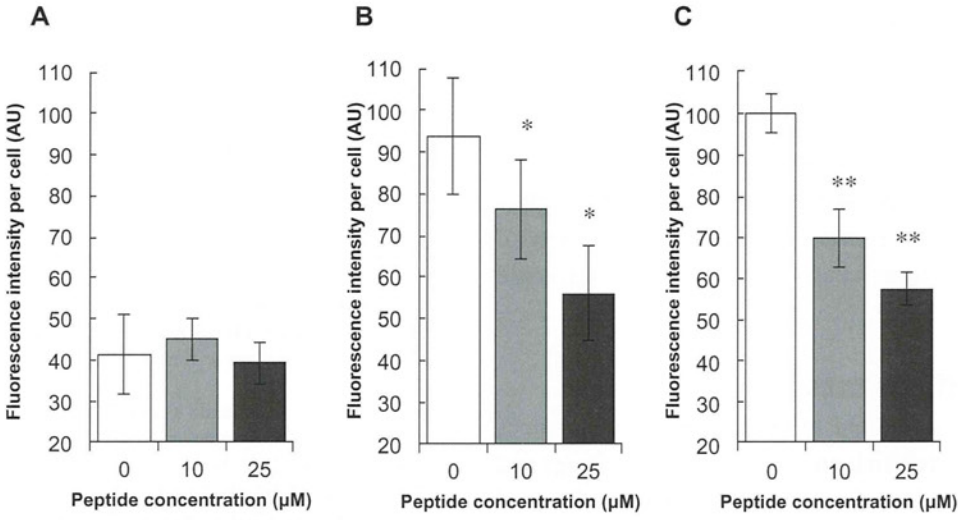

Figure 6 Inhibitory effects of preS1 peptide against transfection of HSPG41C-preS1 nanocages.
Notes: Cell lines HeLa, HepG2, and Huh-7 (**A**–**C**), respectively; statistical significance of differences in fluorescence intensities in absence and presence of preS1 peptide assessed by Student's *t*-test; $*P < 0.05$; $**P < 0.01$.

accumulation of these proteins in hepatic cell cytoplasm but not in the nucleus. On the other hand, the control fluorescent-labeled HSPG41C nanocages were slightly taken up by Huh-7, HepG2, and MCF-7 under the same conditions (Figure 5). Nanoparticles are mostly internalized into cells by endocytosis. Endocytosis can be classified into four groups: clathrin-mediated endocytosis (CME), caveolae-mediated endocytosis, macropinocytosis, and clathrin- and caveolae-independent endocyotosis.[33,34] We investigated the endocytic pathway of HSPG41C-preS1 nanocages using three types of chemical compound that inhibited specific endocytic pathways (Figure S3). Chlorpromazine inhibits CME,[35] amiloride inhibits macropinocytosis,[36] and filipin III inhibits caveolae-mediated endocytosis.[37] When HepG2 cells were treated with amiloride and filipin, 5% and 6% decreases in cellular uptake of HSPG41C-preS1 nanocages were detected compared with untreated cells. Chlorpromazine treatment showed a marked decrease (23%) in the uptake of HSPG41C-preS1 nanocages. These results suggest that HSPG41C-preS1 nanocage was taken up by HepG2 cells by various types of endocytosis, but the main uptake pathway was CME.

To determine the HSPG41C-preS1 nanocage internalization process into hepatoma cells, competition assays using synthetic preS1 peptide, encompassing amino acid residues 21-47 of preS1, were performed. Fluorescent-labeled HSPG41C-preS1 nanocage incorporation in the presence of various concentrations of synthetic preS1 peptides was intensity normalized to 100 for untreated Huh-7 (Figure 6). In the case of human hepatoma-derived cell lines HepG2 and Huh-7, synthetic preS1 peptides inhibited incorporation of labeled HSPG41C-preS1 nanocages in a dose-dependent manner. On the other hand, the presence of synthetic preS1 peptides did not significantly influence interaction between these nanocages and HeLa cells. These results suggested that the cell binding observed for these nanocages was due specifically to the presence of the preS1 moiety on their surfaces and the internalization of the nanocages was achieved by interaction with preS1 receptors on the hepatocyte cell lines.

Conclusion

In summary, genetic incorporation of hepatocyte binding preS1 peptide onto the exterior surface of nanocages conferred cell-specific targeting capabilities to this protein cage architecture. These protein nanocages were efficiently internalized into hepatocyte cell lines, mainly through clathrin-mediated endocytosis, without cytotoxicity, and were localized at cytoplasm. Furthermore, the binding of HSPG41C-preS1 nanocages to HepG2 cells was prevented by synthetic preS1-(21-47) peptide in a dose-dependent manner, suggesting that this sequence could be directly responsible for nanocage attachment to the cellular surface. In fact, it is known that the preS1 domain of HBV is modified with myristic acid at the N-terminal region and that this modification is important for efficient infectivity,[27,28] and thus it appears that it would be necessary to conjugate the HSPG41C-preS1 nanocages with a similar lipid to enhance specificity in hepatocyte targeting in vivo. This strategy was effective for producing suitable nanocages that were directed to and taken up by specific cell types, target organs, or cancer

cells, which is an important development in such applications, as ligand-mediated active binding to sites and cellular uptake are particularly valuable to therapeutic agents that are not easily taken up by cells. Furthermore, these nanocages are self-organized complexes of protein oligomers and possess nanoscale inner cavities, whose three-dimensional architecture can be specified in detail and into which a variety of molecules, including therapeutic or diagnostic agents, could be encapsulated.

Acknowledgments

This work was supported by a Health Labor Sciences Research Grant (Research on Publicly Essential Drugs and Medical Devices) from the Ministry of Health Labor and the Special Coordination Funds for Promoting Science and Technology (SCF funding program "Innovation Center for Medical Redox Navigation"), Japan.

Disclosure

The authors report no conflict of interest in this work.

References

1. Kang JH, Oishi J, Kim JH, et al. Hepatoma-targeted gene delivery using a tumor cell-specific gene regulation system combined with a human liver cell-specific bionanocapsule. *Nanomedicine*. 2010;6(4):583–589.
2. Pridgen EM, Langer R, Farokhzad OC. Biodegradable, polymeric nanoparticle delivery systems for cancer therapy. *Nanomedicine (Lond)*. 2007;2(5):669–680.
3. Sawant RM, Hurley JP, Salmaso S, et al. "SMART" drug delivery systems: double-targeted pH-responsive pharmaceutical nanocarriers. *Bioconjug Chem*. 2006;17(4):943–949.
4. Wang M, Thanou M. Targeting nanoparticles to cancer. *Pharmacol Res*. 2010;62(2):90–99.
5. Brayden DJ. Controlled release technologies for drug delivery. *Drug Discov Today*. 2003;8(21):976–978.
6. Allen TM, Cullis PR. Drug delivery systems: entering the mainstream. *Science*. March 19, 2004;303(5665):1818–1822.
7. Aso S, Ise H, Takahashi M, et al. Effective uptake of N-acetylglucosamine-conjugated liposomes by cardiomyocytes in vitro. *J Control Release*. 2007;122(2):189–198.
8. Khandare J, Minko T. Polymer-drug conjugates: progress in polymeric prodrugs. *Prog Polym Sci*. 2006;31(4):359–397.
9. Toita R, Kang JH, Kim JH, et al. Protein kinase C alpha-specific peptide substrate graft-type copolymer for cancer cell-specific gene regulation systems. *J Control Release*. 2009;139(2):133–139.
10. Tsuchiya A, Naritomi Y, Kushio S, et al. Improvement in the colloidal stability of protein kinase-responsive polyplexes by PEG modification. *J Biomed Mater Res A*. 2012;100(5):1136–1141.
11. Yoshinori M, Masaharu M, Yuri H, Sayoko N, Nao S, Makoto H. Molecular imaging contrast media for visualization of liver function. *Magn Reson Imaging*. 2010;28(5):708–715.
12. Davis ME, Chen ZG, Shin DM. Nanoparticle therapeutics: an emerging treatment modality for cancer. *Nat Rev Drug Discov*. 2008; 7(9):771–782.
13. Flenniken ML, Willits DA, Harmsen AL, et al. Melanoma and lymphocyte cell-specific targeting incorporated into a heat shock protein cage architecture. *Chem Biol*. 2006;13(2):161–170.
14. Kasuya T, Kuroda S. Nanoparticles for human liver-specific drug and gene delivery systems: in vitro and in vivo advances. *Expert Opin Drug Deliv*. 2009;6(1):39–52.
15. Sao K, Murata M, Fujisaki Y, et al. A novel protease activity assay using a protease-responsive chaperone protein. *Biochem Biophys Res Commun*. 2009;383(3):293–297.
16. Uchida M, Klem MT, Allen M, et al. Biological containers: protein cages as multifunctional nanoplatforms. *Adv Mater*. 2007;19(8): 1025–1042.
17. MacRae TH. Structure and function of small heat shock/alpha-crystallin proteins: established concepts and emerging ideas. *Cell Mol Life Sci*. 2000;57(6):899–913.
18. Sun Y, MacRae TH. Small heat shock proteins: molecular structure and chaperone function. *Cell Mol Life Sci*. 2005;62(21): 2460–2476.
19. Sao K, Murata M, Umezaki K, et al. Molecular design of protein-based nanocapsules for stimulus-responsive characteristics. *Bioorg Med Chem*. 2009;17(1):85–93.
20. Kim DR, Lee I, Ha SC, Kim KK. Activation mechanism of HSP16.5 from Methanococcus jannaschii. *Biochem Biophys Res Commun*. 2003;307(4):991–998.
21. Kim R, Kim KK, Yokota H, Kim SH. Small heat shock protein of Methanococcus jannaschii, a hyperthermophile. *Proc Natl Acad Sci U S A*. 1998;95(16):9129–9133.
22. Nakamoto H, Vigh L. The small heat shock proteins and their clients. *Cell Mol Life Sci*. 2007;64(3):294–306.
23. Kaiser CR, Flenniken ML, Gillitzer E, et al. Biodistribution studies of protein cage nanoparticles demonstrate broad tissue distribution and rapid clearance in vivo. *Int J Nanomedicine*. 2007;2(4):715–733.
24. Kim KK, Kim R, Kim SH. Crystal structure of a small heat-shock protein. *Nature*. 1998;394(6693):595–599.
25. Argnani R, Boccafogli L, Marconi PC, Manservigi R. Specific targeted binding of herpes simplex virus type 1 to hepatocytes via the human hepatitis B virus preS1 peptide. *Gene Ther*. 2004;11(13): 1087–1098.
26. De Falco S, Ruvoletto MG, Verdoliva A, et al. Cloning and expression of a novel hepatitis B virus-binding protein from HepG2 cells. *J Biol Chem*. 2001;276(39):36613–36623.
27. Paran N, Cooper A, Shaul Y. Interaction of hepatitis B virus with cells. *Rev Med Virol*. 2003;13(3):137–143.
28. Barrera A, Guerra B, Notvall L, Lanford RE. Mapping of the hepatitis B virus pre-S1 domain involved in receptor recognition. *J Virol*. 2005;79(15):9786–9798.
29. Glebe D, Urban S. Viral and cellular determinants involved in hepadnaviral entry. *World J Gastroenterol*. 2007;13(1):22–38.
30. Neurath AR, Kent SB, Strick N, Parker K. Identification and chemical-synthesis of a host cell receptor binding site on hepatitis B virus. *Cell*. 1986;46(3):429–436.
31. Qiao M, Macnaughton TB, Gowans EJ. Adsorption and penetration of hepatitis B virus in a nonpermissive cell line. *Virology*. 1994;201(2):356–363.
32. Dash S, Rao KV, Panda SK. Receptor for Pre-Sl(21-47) component of hepatitis B virus on the liver cell: role in virus cell interaction. *J Med Virol*. 1992;37(2):116–121.
33. Sahay G, Alakhova DY, Kabanov AV. Endocytosis of nanomedicines. *J Control Release*. 2010;145(3):182–195.
34. Conner SD, Schmid SL. Regulated portals of entry into the cell. *Nature*. 2003;422(6927):37–44.
35. Wang L-H, Rothberg KG, Anderson RGW. Mis-assembly of clathrin lattices on endosomes reveals a regulatory switch for coated pit formation. *J Cell Biol*. 1993;123(5):1107–1117.
36. Hewlett LJ, Prescott AR, Watts C. The coated pit and macropinocytic pathways serve distinct endosome populations. *J Cell Biol*. 1994;124(5):689–703.
37. Lamaze C, Schmid SL. The emergence of clathrin-independent pinocytic pathways. *Curr Opin Cell Biol*. 1995;7(4):573–580.

Supplementary figures

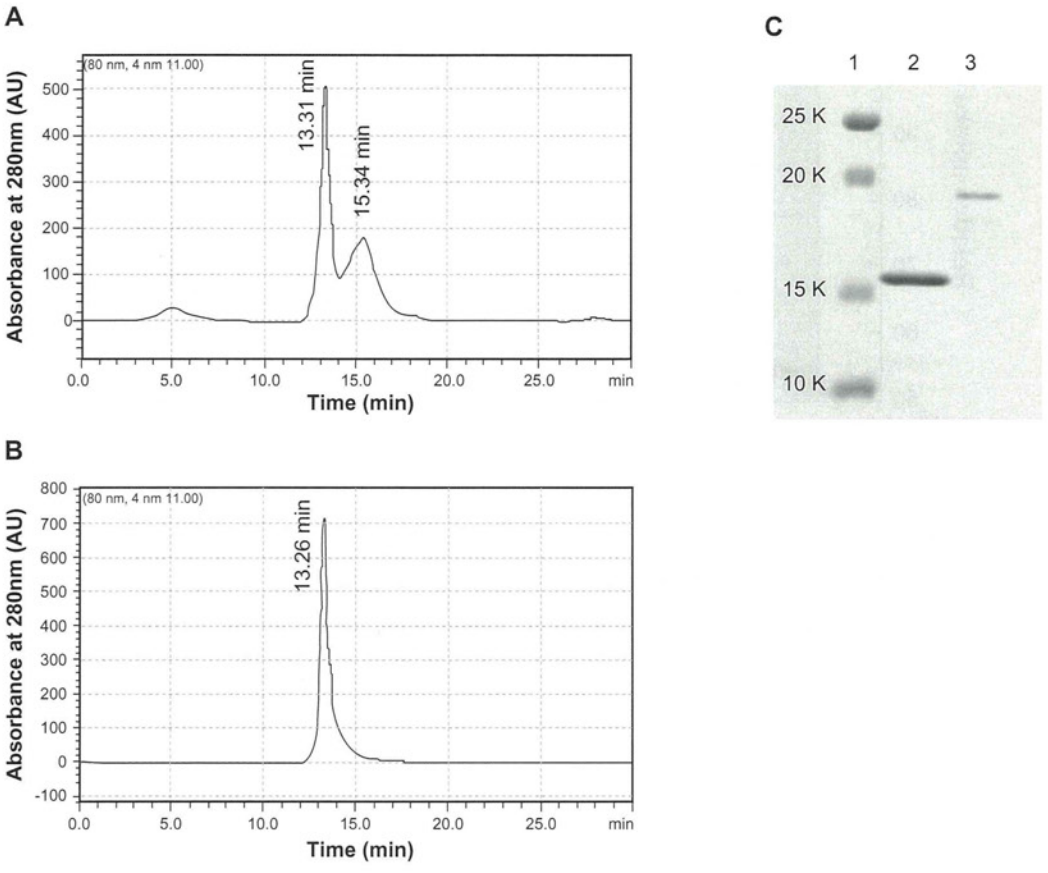

Figure S1 Gel permeation chromatography purification of HSPG41C nanocages and HSPG41C-preS1 nanocages. GHSPG41C nanocages (**A**); HSPG41C-preS1 nanocages (**B**). The peaks observed at 13.31 minutes in (**A**) and 13.26 minutes in (**B**) were collected individually. The collected fractions were then analyzed by SDS-PAGE using 12% gel according to the standard protocol (**C**).
Note: Lane 1, molecular weight standards; lane 2, HSPG41C nanocages; lane 3, HSPG41C-preS1 nanocages.
Abbreviation: SDS-PAGE, sodium dodecyl sulfate polyacrylamide gel electrophoresis.

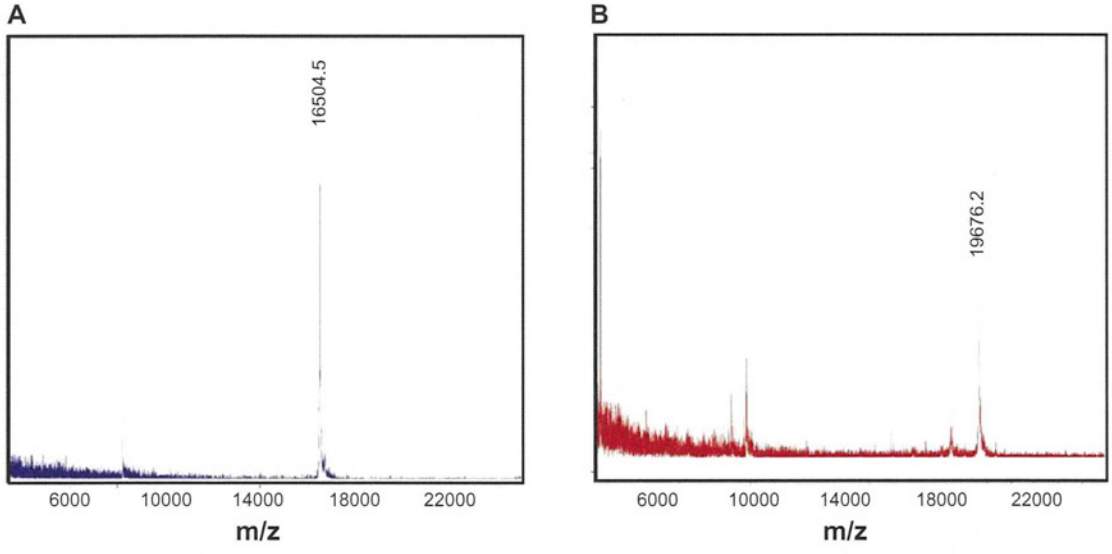

Figure S2 MALDI-TOF mass spectrum of HSPG41C nanocages and HSPG41C-preS1 nanocages. GHSPG41C nanocages (**A**); HSPG41C-preS1 nanocages (**B**).
Abbreviation: MALDI-TOF, matrix-assisted laser desorption/ionization time of flight.

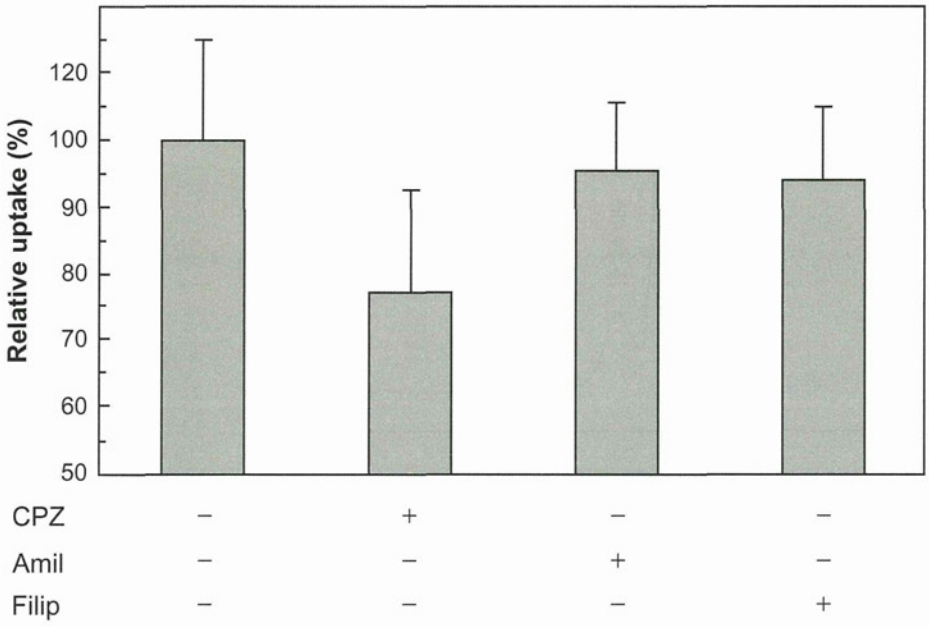

Figure S3 Inhibition of cellular uptake of HSPG41C-preS1 nanocages by endocytosis inhibitors.

Notes: HepG2 cells were harvested on poly-L-lysine-coated 48-well plates at an initial density of 50,000 cells/well and grown overnight. Cells were treated with DMEM containing chlorpromazine (10 μg/mL), amiloride (500 μM), or filipin III (10 μg/mL) for 1 hour (all from Sigma-Aldrich, St Louis, MO). Then 84 nM of fluorescent-labeled HSPG41C-preS1 nanocages solution containing the above inhibitors was added to cells. Two hours after transfection, cells were rinsed three times with PBS and then lysed in lysis buffer (pH 7.5, 20 mM Tris-HCl, 2 mM EDTA, and 0.05% Triton-X 100). Lysate solutions were replaced on black-bottomed 96-well plates and the fluorescence intensity of each sample measured using a Microplate Reader (ARVO MX 1420; Perkin Elmer Inc, Waltham, MA). Data are means ± SEM of three independent experiments.

Abbreviations: CPZ, chlorpromazine; Amil, amiloride; Filip, filipin; DMEM, Dulbecco's Modified Eagle's Medium; PBS, phosphate buffered saline; HCl, hydrochloride; EDTA, ethylenediaminetetraacetic acid; SEM, standard error of the mean.

Bioconjugate Chemistry

Technical Note

pubs.acs.org/bc

Development of Human Hepatocellular Carcinoma Cell-Targeted Protein Cages

Riki Toita,[†,⊥] Masaharu Murata,*[,†,‡,∥] Shigekazu Tabata,[‡] Kana Abe,[∥] Sayoko Narahara,[†] Jing Shu Piao,[‡] Jeong-Hun Kang,[#] and Makoto Hashizume[†,‡,∥]

[†]Innovation Center for Medical Redox Navigation, [‡]Department of Advanced Medical Initiatives, Faculty of Medical Sciences, and [∥]Center for Advanced Medical Innovation, Kyushu University, 3-1-1 Maidashi, Higashi-ku, Fukuoka 812-8582, Japan

[#]Department of Biomedical Engineering, National Cerebral and Cardiovascular Center Research Institute, 5-7-1 Fujishirodai, Suita, Osaka 565-8565, Japan

ABSTRACT: We described herein a human hepatocellular carcinoma (HCC) cell-targeted protein cage for which the HCC-binding peptide termed SP94 was modified at the surface of a naturally occurred heat shock protein (Hsp) cage. Six types of HCC-targeted Hsp cages were chemically synthesized using two types of heterobifunctional linker ($SM(PEG)_n$) with different lengths and two types of SP94 peptide, which contained a unique Cys residue at the N- or C-terminus of the peptide. These Hsp cages were characterized using matrix-assisted laser desorption/ionization-time-of-flight mass spectrometry (MALDI-ToF MS) analyses, sodium dodecylsulfate–polyacrylamide gel electrophoresis (SDS-PAGE) analyses, and dynamic light scattering (DLS) measurement. Fluorescence microscopic observations revealed that all the engineered protein cages bind selectively to HCC cells but not to the other cell lines tested (including normal liver cell). Moreover, the number of SP94 peptides on Hsp cages, conjugation site of SP94 peptide, and linker length between a Hsp cage and a SP94 peptide had important effects upon the binding of engineered Hsp cages to HCC cells. An engineered Hsp cage conjugated to the N-terminus of SP94 peptide via a longer linker molecule and containing high SP94 peptide levels showed greater binding toward HCC cells. Surprisingly, through optimization of these three factors, up to 10-fold greater affinity toward HCC cells was achieved. These results are critically important not only for the development of HCC cell-targeting devices using SP94 peptide, but also to create other cell-targeting materials that utilize other peptide ligands.

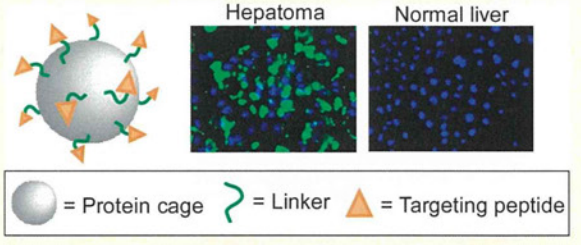

INTRODUCTION

Hepatocellular carcinoma (HCC) is one of the most common types of malignant tumors worldwide. It is the fifth leading cause of cancer death, and is associated with a relatively low prevalence of survival at 5 years.[1] Systemic chemotherapies have been thought to be the most promising strategies for patients with HCC.[2−4] However, many of these conventional chemotherapies have not been shown to improve survival, primarily because HCC is highly resistant against such chemotherapies.[2−4] In addition, many conventional antitumor agents do not selectively kill HCC cells, which can lead to undesirable side effects.[3] Many researchers have therefore attempted to develop tumor-selective carriers (e.g., polymers, liposomes, proteins) for drug delivery system (DDS) based mainly on active targeting strategies (e.g., folic acid, peptide ligands, and antibody-modification with carriers).[5−7]

Recently, a short peptide ligand termed SP94 (peptide sequence: SFSIIHTPILPL) was discovered by using an *in vivo* phase display technique, and was shown to bind selectively to various types of HCC cells.[8] Moreover, SP94-displayed liposome-containing chemotherapeutic agents exhibited much higher affinity toward various types of HCC cells compared with normal cells (including normal hepatocytes, endothelial cells, and immune cells) and killed HCC cells.[9] Thus, SP94 peptide could be useful as a HCC cell-targeted ligand and can be available for developing HCC-targeted DDS. In general, compared with antibodies, peptide ligands have advantages such as easier synthesis, lower expense, and lower immunogenesis. However, the effects of peptide conjugation methodologies (e.g., peptide content, site of peptide conjugation, and effect of linker length between peptide and carriers on affinity of engineered carriers toward HCC cells) have not been thoroughly investigated, even though these factors will be very important for the development of effective drug carriers.

In this study, we described a human HCC-targeted nanoparticle, which was chemically modified SP94 peptides at the exterior of the nanoparticle (Figure 1A). As a model nanoparticle, we focused on small heat shock protein 16.5 (Hsp), a naturally occurring protein in *Methanococcus jannaschii*, which forms a "cage" structure through self-assembly of 24 subunit proteins (i.e., outer size and inner size are 12 and 6.5 nm, respectively) (Figure 1A).[10] Hsp is attractive as a biomedical tool for delivery of therapeutics, imaging device, and sensing material due to its biocompatibility, monodispersed

Received: January 13, 2012
Revised: April 10, 2012
Published: May 23, 2012

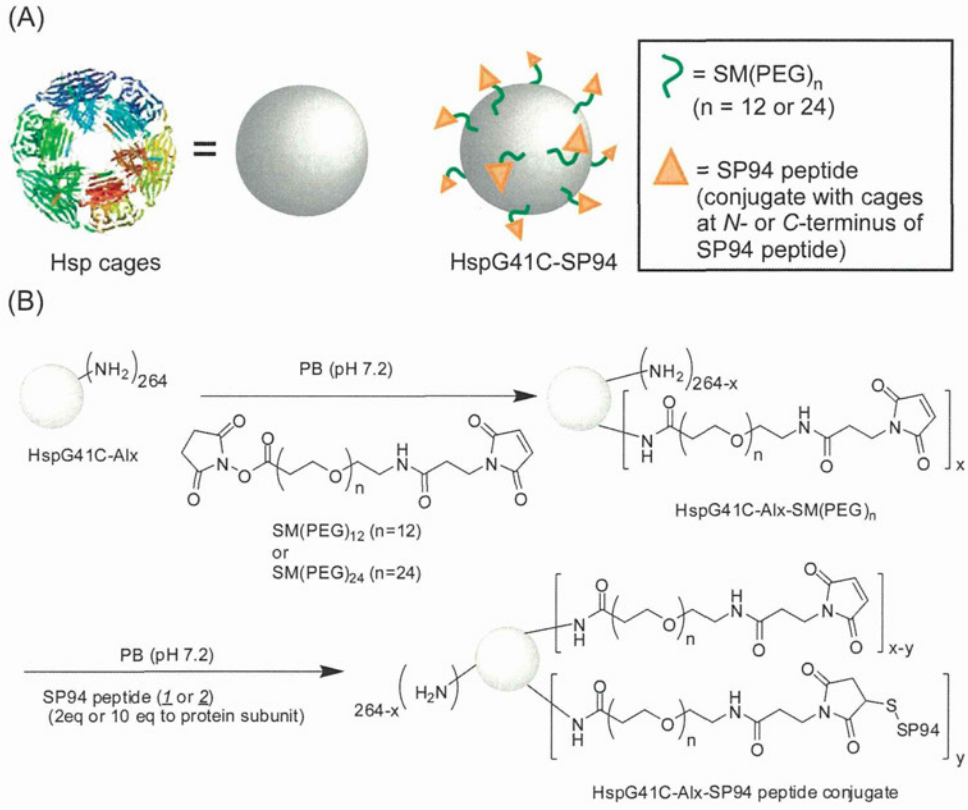

Figure 1. (A) SP94-modified Hsp cage (schematic). An Hsp cage consisted of 24 protein subunits with a molecular weight of 16.5 kDa, and formed a hollow-shaped structure. (B) Synthetic scheme of HspG41C–SP94 peptide conjugates.

formation, robust structure, easy acquisition from *Escherichia coli*, and easy functionalization through chemical and genetic strategies.[11−20] However, Hsp does not have sufficient specificity for cells or tissues, which is a major obstacle to its application as a drug carrier or imaging device. Therefore, providing specificity toward certain cells or tissues for Hsp is very important for disease treatment and diagnostic imaging.

We first synthesized six types of engineered "protein cages" which were different in (i) SP94 peptide contents, (ii) conjugation site of SP94 peptide, and (iii) linker length between an Hsp cage and an SP94 peptide. Synthesized Hsp cage-SP94 peptide conjugates were analyzed using matrix-assisted laser desorption/ionization−time-of-flight mass spectrometry (MALDI-ToF MS) analyses, sodium dodecylsulfate−polyacrylamide gel electrophoresis (SDS-PAGE) analyses, and dynamic light scattering (DLS) measurement. Observation of fluorescence microscopic images revealed that all of the engineered Hsp cages bind selectively to human HCC cells (HepG2 and Huh-7 cells) but not to other cell lines including human cervical carcinoma (HeLa) cells and rat normal hepatocyte (RLN-8). Interestingly, the level of binding to HCC cells of engineered protein cages was changed appreciably according to (i) peptide content, (ii) conjugation site of peptide, and (iii) linker length. These results provide useful information to enhance cellular uptake of peptide ligand-fabricated nanoparticles by simply changing chemical conjugation strategy of peptide ligands.

■ EXPERIMENTAL PROCEDURES

Expression and Purification of HspG41C Cages. The pET21a(+) vector-encoded HspG41C mutant in which Gly residue at position 41 of wild-type Hsp was substituted with a Cys residue was prepared by polymerase chain reaction (PCR)-mediated mutagenesis using the appropriate primers. The success of mutagenesis was confirmed by DNA sequencing. HspG41C mutant protein was expressed from *E. coli*, and was purified using anion exchange chromatography and size exclusion chromatography (SEC). BL21 Gold(DE3) (Novagene, Tokyo, Japan) was used as a strain for HspG41C.

E. coli containing the pET21a(+) plasmid vector were grown in 2 × YT medium containing 100 μg/mL of ampicillin at 37 °C. When the optical density (OD) at 600 nm of the culture medium reached between 0.5 and 0.6, expression of a recombinant protein was induced with 1 mM of isopropyl-β-D-thiogalactopyranoside (IPTG) (Wako Pure Chemical Ind. Ltd., Osaka, Japan) for 4 h at 37 °C. After collection by centrifugation, cells were suspended in 25 mM KH_2PO_4 solution (containing 1 mM ethylenediamine tetraacetic acid (EDTA) and 2 mM dithiothreitol (DTT), pH 7.0) and stored at −80 °C until purification. Cell suspensions were sonicated to disrupt the cell membrane. Cell lysate solutions were then centrifuged at 15 000 rpm for 30 min at 4 °C and then supernant collected. Proteins were purified using a HiLoad 26/10 QSepharose HP anion exchange column (GE Healthcare, Buckinghamshire, UK) and a SEC column (TSKgel G3000SW; Tosoh, Tokyo, Japan). Purification was confirmed by 15% SDS-PAGE analyses.

Synthesis of Alexa488-Modified HspG41C (HspG41C-Alx). For modification of fluorophores on the interior of HspG41C, HspG41C (2.5 mg, 152 nmol Cys residues) was reacted with Alexa-Fluor 488 C_5-maleimide (0.13 mg, 182 nmol) (Invitrogen, Carlsbad, CA, USA) in 0.1 M phosphate buffer (PB; pH 7.2) for 2 h at room temperature. The reactant was further incubated for 20 h at 4 °C. Unreacted Alexa-Fluor

dx.doi.org/10.1021/bc300015f | Bioconjugate Chem. 2012, 23, 1494−1501

488 C_5-maleimide was removed by ultrafiltration using Amicon Ultra Centrifugal Filters with MWCO 100 000 (Millipore, Tokyo, Japan). The success of Alexa488 modification to HspG41C was confirmed using MALDI-ToF MS analyses. Modified amounts of Alexa488 in HspG41C-Alx cages were calculated from absorbance data of Alexa488 (ε_{495} = 73 000 cm^{-1} M^{-1}).

Synthesis of SP94 Peptide-Modified HspG41C-Alx. To introduce maleimide groups to Hsp cages, heterobifunctional poly(ethylene glycol) linkers possessing succinimidyl and maleimide groups at the end of linkers ($SM(PEG)_n$; n = 12 or 24) (Thermo Scientific, Kanagawa, Japan) were used. HspG41C-Alx was modified with $SM(PEG)_n$ (50× excess of the protein monomer) through amide bonds in PB (0.1 M, pH 7.2) for 2 h at room temperature, followed by removal of unreacted $SM(PEG)_n$ by ultrafiltration as described above to obtain HspG41C-Alx-$SM(PEG)_n$-containing maleimide groups.

For modification of SP94 peptide, two types of SP94 peptides containing a Cys residue at the N-terminus or C-terminus were prepared; sequences of peptides **1** and **2** were Ac-CGGSFSIIHTPILPL-NH_2 and Ac-SFSIIHTPILPLGGC-NH_2, respectively (the underline indicates the SP94 peptide sequence). HspG41C-Alx-$SM(PEG)_n$ and SP94 peptides (2 or 10 equiv to protein monomer) were dissolved in PB (0.1 M, pH 7.2) and stirred for 6 h at room temperature, and allowed to stand for 20 h at 4 °C. The mixture was purified by ultrafiltration as described above.

MALDI-ToF MS Analyses. Measurement of the molecular weight of PEG-modified HspG41C cages was performed by MALDI-ToF MS analysis using Autoflex Speed (Bruker Daltonics Inc., Billerica, MA, USA), and sinapinic acid (Bruker Daltonic Inc.) was used as a matrix.

SDS-PAGE Analysis. SDS-PAGE was performed using 15% SDS-PAGE gel (Wako Pure Chemical. Ind.). Sample bands were imaged by the fluorescence of Alexa488 bound to each protein cage using a Typhoon FLA9000 Biomolecular Imager (GE Healthcare). Fluorescence images were analyzed using ImageQuant TL (GE Healthcare). Modified amounts of $SM(PEG)_n$ and SP94 peptides in Hsp cages were determined from band intensity of SDS-PAGE analysis as described in previous stuides.[16,21] Briefly, band fluorescence intensities of each modified Hsp cage were measured quantitatively using ImageQuant TL, and then contents of $SM(PEG)_n$ and SP94 peptides were calculated from the fluorescence intensity ratios of each band.

Measurement of the Size of SP94-Modified HspG41C Cages by DLS. All samples and buffer solutions were filtered using Ultrafree-MC with pore sizes of 0.22 μm (Millipore, Tokyo, Japan) before DLS measurement. Sizes of protein cages (0.1 mg/mL) were measured thrice using a Zeta-Sizer Nano ZS Analyzer (Malvern, UK) at the detection angles of 173° and temperature of 25 °C. The 633 nm wavelength from a He−Ne laser was used as an incident beam.

Cell Culture. Human HCC (Huh-7 and HepG2), human cervical carcinoma HeLa, and rat normal liver cell RLN-8 cells were cultured in the appropriate medium containing 10% fetal bovine serum (FBS), 100 U/mL penicillin, 100 μg/mL streptomycin, and 0.25 μg/mL amphotericin-B (all from Gibco, NY, USA) in a humidified atmosphere of 5% CO_2 and 95% air at 37 °C. Dulbecco's modified Eagle's medium (DMEM) was used for cultivation of Huh-7 and HepG2 cells, Eagle's minimal essential medium (EMEM) containing nonessential amino acids for HeLa cells and minimal essential medium α (MEMα) for RLN-8 cells (all from Wako) were used.

Fluorescence Microscopic Observation. Cells were seeded on 96-well culture plates with an initial cell density of 10 000/well and cultured for 1 day in 100 μL of the appropriate medium containing 10% FBS. Final concentrations of Hsp cages were adjusted to 40 nM (1 μM of subunit protein) by Opti-MEM (Gibco) and 100 μL of diluted Hsp cages was added to the each well. After incubation for 24 h, the medium was changed to fresh Opti-MEM containing 5 μg/mL of Hoechst 33342 (Dojindo, Kumamoto, Japan) and incubated for 1 h. Fluorescence images were obtained using the fluorescence microscope BZ-9000 (Keyence, Osaka, Japan). For blocking the binding of Hsp cages to target receptors, excessive amounts of free SP94 peptides (100 μM) were added to cells with Hsp cages.

Fluorescence Measurement of Cellular Uptake of HspG41C-$SM(PEG)_n$-SP94 Peptide Conjugates. Huh-7 and HepG2 cells were harvested on 96-well plates with an initial cell density of 10 000/well, and cultured for 1 day. Fifty microliters of each protein cage diluted with Opti-MEM (4 nM) were added to each well. After incubation for 24 h, cells were rinsed twice with phosphate-buffered saline (PBS)(−) and then lysed in 100 μL of buffer (pH 7.5, 20 mM Tris-HCl, 2 mM EDTA, and 0.05% Triton-X 100). Lysate solutions were replaced on black-bottomed 96-well plates, and the fluorescence intensity of each sample measured using a Microplate Reader (ARVO MX 1420; Perkin-Elmer Inc., Waltham, MA, USA).

Cell Viability Assay after Adding Free SP94 Peptides to Huh-7 Cells. Huh-7 cells were harvested on 96-well plates at an initial cell density of 10 000 cells/well and grown overnight at 37 °C overnight. After adding SP94 peptides (3−300 μM) dissolved in Opti-MEM to cells, the cells were incubated at 37 °C for 24 h. Cell viability was measured using a CellTiter-Glo luminescent cell viability assay kit (Promega, Madinson, WI, USA) according to the manufacture's protocol. Luminescence intensity was measured using a Microplate Reader (ARVO MX 1420; Perkin-Elmer Inc., Waltham, MA, USA).

Fluorescence Microscopic Observation of Subcellular Localization of HspG41C-$SM(PEG)_n$-SP94 Peptide Conjugates. Huh-7 cells were harvested on 48-well plates at initial density of 10 000 cells/well and grown overnight at 37 °C overnight. After adding HspG41C-$SM(PEG)_n$-SP94 peptide conjugates (40 nM) to cells, the cells were incubated at 37 °C for 24 or 48 h. Acidic organelles and nuclei were stained by LysoTracker Red DND-99 (Invitrogen, Carlsbad, CA, USA) and Hoechst 33342 (Dojindo), respectively. Fluorescence images were obtained using the fluorescence microscope BZ-9000 (Keyence, Osaka, Japan).

■ RESULTS AND DISCUSSION

Synthesis and Characterization of HCC Targeted Peptide- and Fluorophore-Modified HspG41C Cages. The synthetic scheme of HspG41C-Alx-SP94 is described in Figure 1B. HspG41C was labeled with Alexa488-maleimide at the interior of HspG41C cages via thioether bonds between a unique Cys residue of HspG41C and a maleimide group of Alexa488 (HspG41C-Alx). Binding of Alexa488 to HspG41C was identified by MALDI-ToF MS analyses (Figure 2A). From absorbance of Alexa488 at 495 nm (ε_{495} = 73 000 cm^{-1} M^{-1}), we estimated that 22 molecules of Alexa488 were modified with each HspG41C-Alx cage (0.93 molecules/monomer protein).